



Efficient blue lighting materials based on truxene-cored anthracene derivatives for electroluminescent devices

Jinhai Huang^a, Bin Xu^a, Jian-Hua Su^{a,*}, Chin H. Chen^b, He Tian^{a,*}

^aKey Laboratory for Advanced Materials and Institute of Fine Chemicals, East China University of Science & Technology, Shanghai 200237, China

^bCenter for Advanced Luminescence Materials, Department of Chemistry, Hong Kong Baptist University, Kowloon Tong, Hong Kong, China

ARTICLE INFO

Article history:

Received 7 June 2010

Received in revised form 12 July 2010

Accepted 16 July 2010

Available online 22 July 2010

ABSTRACT

A new series of anthracene derivatives containing a truxene moiety as the core have been synthesized and characterized. They emit in the blue region with excellent solution fluorescence quantum yields and possess high thermal decomposition temperature ($T_d > 458$ °C). Typical electroluminescence performance was demonstrated by 2-[10-(4-(1-naphthyl)phenyl)anthracene-9-yl]-5,5',10,10',15,15'-hexaethyltruxene (NPAT) as the blue lighting material in the OLED with structure of ITO/CFx/NPAT/TPBI or Alq₃/LiF/Al, where TPBI and Alq₃ are 1,3,5-tri(*N*-phenylbenzimidazol-2-yl)-benzene and tris(8-hydroxyquinolino) aluminum, respectively. Additionally, the effects of the different thickness of the different electron transporting layers on the device performance were investigated.

© 2010 Elsevier Ltd. All rights reserved.

1. Introduction

Organic light-emitting devices (OLEDs) have drawn great scientific and commercial attention in the past decades, due to their potential applications in full-color, flat-displays as well as solid-state lighting.¹ Blue emission materials play a particularly important role in the development of OLEDs, which can be utilized to generate light of other colors by energy cascade to a suitable emissive dopant.² Compared to the efficient and stable green and red emitter, efficient blue OLED remains to be a challenge since sufficiently wide band gap of highly efficient and stable blue luminescent materials are still rare. Although intensive study has been devoted to developing new blue fluorescence materials, only a limited number of them can achieve both color purity and stability in OLEDs with good performance.

Because of the unusual photoluminescence and electroluminescence properties and excellent electrochemical properties, anthracene derivatives have been intensively used as blue emission materials in OLEDs. By introducing different bulky aryl groups at the C-9 and -10 positions, plenty of stable and tunable emission materials are conveniently synthesized.³ Recently, Wu and co-workers⁴ have reported anthracene derivative end-capped with fluorene groups from which an external quantum efficiency of 5.1% and EL efficiency of 5.6 cd A⁻¹ with a saturated blue CIE_(x,y) of (0.15, 0.12) in a non-doped system has been achieved. Xia and co-workers⁵ have

reported unsymmetrical indene-substituted anthracene doped diphenyl-[4-(2-[1,1'; 4',1''] terphenyl-4-yl-vinyl)-phenyl]-amine with a maximum power efficiency of 8.39 lm/W (7.6 cd A⁻¹ at 2.90 V) with a pure blue emission at CIE_(x,y) of (0.14, 0.18). These encouraging results will accelerate the development of OLEDs and its ongoing commercialization activities.

Truxene (10,15-dihydro-5*H*-diindenol[1,2-*a*:1',2'-*c*]-fluorene) is a planar heptacyclic polyarene,⁶ which can be formally regarded as a C₃-symmetrically fused fluorene trimer. Because the truxene moiety by virtue of its unique three-dimensional topology is easily functionalized by different substituents at C-2, -7, -12 positions and at C-5, -10, -15 positions, as well, it has been intensively developed as an attractive building block and starting material for various functional organic materials, such as OLEDs,⁷ liquid crystals,⁸ two-photon absorption,⁹ fluorescence sensor,¹⁰ organic solar cells,¹¹ as well as large π -conjugation dendrimer macromolecular.¹² Thereby, the abundant derivatives including fantastic electro-optical properties largely extend the truxene utilization in various technological. Moreover, the modified truxene derivatives exhibit high glass-transition temperature (T_g) and excellent thermal stabilities as well as high performance for OLEDs.^{7b,f}

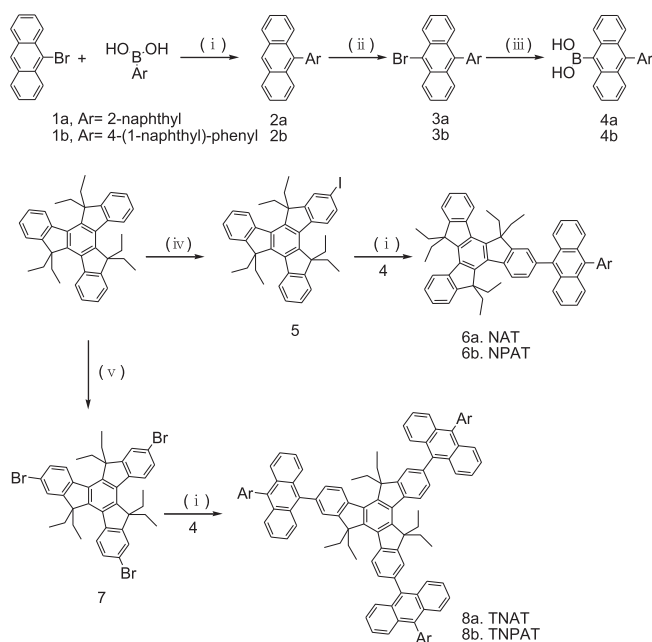
In this paper, we linked the truxene and anthracene moiety through Suzuki cross-coupling reactions to synthesize four compounds with one anthracene moiety arm and three arms at the truxene core as the promising candidates for blue host materials in OLEDs. In addition, six ethyl substituents were introduced at C-5, -10, -15 positions of truxene core, which can not only efficiently improve the solubility of the target compounds, but also could alleviate intermolecular interactions in the solid state.

* Corresponding authors. Tel.: +86 21 64252756; fax: +86 21 64252288 (H.T.); tel./fax: +86 21 64252288 (J.-H.S.); e-mail addresses: bbsjh@ecust.edu.cn (J.-H. Su), tianhe@ecust.edu.cn (H. Tian).

2. Result and discussion

2.1. Synthesis and characterization

The synthetic routes and the chemical structures of the four representative target compounds NAT, NPAT, TNAT, and TNPAT were shown in Scheme 1. 9-(Aryl)-anthracene was easily obtained from 9-bromo-anthracene and aryl boronic acid through Suzuki coupling reactions. The 9-(aryl)anthracene boronic acid was obtained by reacting 9-bromo-10-(aryl)anthracene and *n*-BuLi and trimethylborate in good yield. The hexa(ethyl)truxene was efficiently prepared according to the literatures.¹³ Corresponding bromide and iodide were afforded by reacting truxene with bromine and iodine, respectively. The Suzuki coupling reaction was also employed in the synthesis of the target compounds with the corresponding bromide and iodide with anthracene boronic acid. All compounds have good solubility in common solvents due to the hexaethyl groups and were available purified with the silica column chromatography or recrystallization. The synthesized compounds were confirmed by NMR spectroscopy and mass spectrometry.



Scheme 1. The synthetic routes of the four representative compounds. Regents and conditions: (i) Pd(PPh₃)₄, 2 M K₂CO₃, THF, reflux; (ii) NBS, DMF, 50 °C, overnight; (iii) *n*-BuLi, THF, −78 °C, (CH₃O)₃B, HCl, 12 h; (iv) HIO₃, I₂, CH₃COOH, H₂SO₄, H₂O, CCl₄, 80 °C, 5 h; (v) Br₂, CH₂Cl₂, 25 °C, overnight.

2.2. Thermal properties

We carried out thermogravimetric analysis (TGA) and differential scanning calorimetry (DSC) to determine the thermal properties of the synthesized materials. TGA indicates that NAT, NPAT, TNAT, TNPAT exhibit decomposition temperatures (T_d ; corresponding to

5% weight loss) as high as 458, 480, 504, and 525 °C, respectively. As shown in Figure S1 and Table 1, T_d increases obviously as the molecular weight increases. In the DSC curves of these materials, no melting point temperatures (T_m) and glass-transition peaks (T_g) were observed although the compounds were heated to 400 °C. The excellent thermal properties with high T_d and T_m will readily improve the OLEDs performance and lifetime during operation.

2.3. Photophysical properties

The UV and PL spectra of the truxene-cored anthracene derivatives in dilute dichloromethane solution as well as in the solid thin film spin-coated with PMMA on quartz plates were measured as shown in Figure 1. A summary of photophysical data of these compounds was also given in Table 1. All absorption spectra in dichloromethane solution similarly exhibit the characteristic vibrational structures of the isolated anthracene groups (peaks at around 399 nm, 377 nm, 360 nm) and the truxene core (peaks of NAT and NPAT at 307 nm, while the other compounds at 312 nm). Additionally, the maximum absorption peaks at around 262 nm are attributable to the $\pi-\pi^*$ transition of the naphthalene units. Upon UV excitation at 380 nm, all the materials in dilute dichloromethane solution exhibit almost identical fluorescent emission at 435 nm. The maximum PL peaks of the solid state of NAT, NPAT, TNAT, TNPAT are 439, 442, 451, and 457 nm, respectively. That suggests that the PL spectra of the solid thin film of these four compounds are red-shifted compared with those in solution owing to the solid-state effect.^{3c,14} The PL spectra of NAT and NPAT both in solution and film are quite close, while TNAT and TNPAT, respectively, show red-shifted about 16 nm and 22 nm. The interesting phenomena indicated the more substituents at the truxene core would extend the π -electronic conjugation in the solid states.

2.4. Electrochemical properties

In order to measure the HOMO value of the synthesized compounds, cyclic voltammetry (CV) analyses were carried out in dichloromethane with 0.1 M Bu₄NPF₆ as the supporting electrolyte versus a Ag/AgCl platinum disk as the working electrode and platinum wire as the counter as the counter electrode. The LOMO energy levels were estimated merely from the absorption edge of the optical absorption spectra. The CV curve was shown in Figure 2 and the electrochemical data were listed in Table 1. Because of the presence of the anthracene moiety,¹⁵ all the compounds present the almost identical HOMO levels (5.55–5.58 eV) with different π -conjugation substitutes.

2.5. Electroluminescent properties

To investigate the electroluminescent properties of the truxene-cored anthracene compounds, we chose NPAT with high solution quantum yield for the OLED fabrication. Four devices using the NPAT as blue lighting material were fabricated with the configurations: **1** ITO/NPB (50 nm)/NPAT (40 nm)/Alq₃ (30 nm)/LiF (1 nm)/Al (100 nm); **2** ITO/NPB (50 nm)/NPAT (40 nm)/Alq₃ (15 nm)/LiF

Table 1
Physical properties of anthracene derivatives

Compound	$\lambda_{\max}(\text{abs})^a$ (nm)	$\lambda_{\max}(\text{em})^a$ (nm)	$\lambda_{\max}(\text{em})^b$ (nm)	Φ_f^c	E_g (eV)	T_d (°C)	HOMO (eV)	LUMO (eV)
NAT	262, 307, 277, 398	437	439	0.70	2.98	458	5.55	2.57
NPAT	263, 307, 378, 397	435	442	0.77	2.98	480	5.55	2.57
TNAT	261, 312, 377, 399	435	451	0.70	2.97	504	5.58	2.61
TNPAT	262, 312, 377, 399	435	457	0.74	2.96	525	5.57	2.61

^a Measured in CH₂Cl₂ solution.

^b Measured in solid state.

^c PL quantum yield relative to 9,10-diphenylanthracene(DPA) in cyclohexane ($\Phi_f=0.90$).

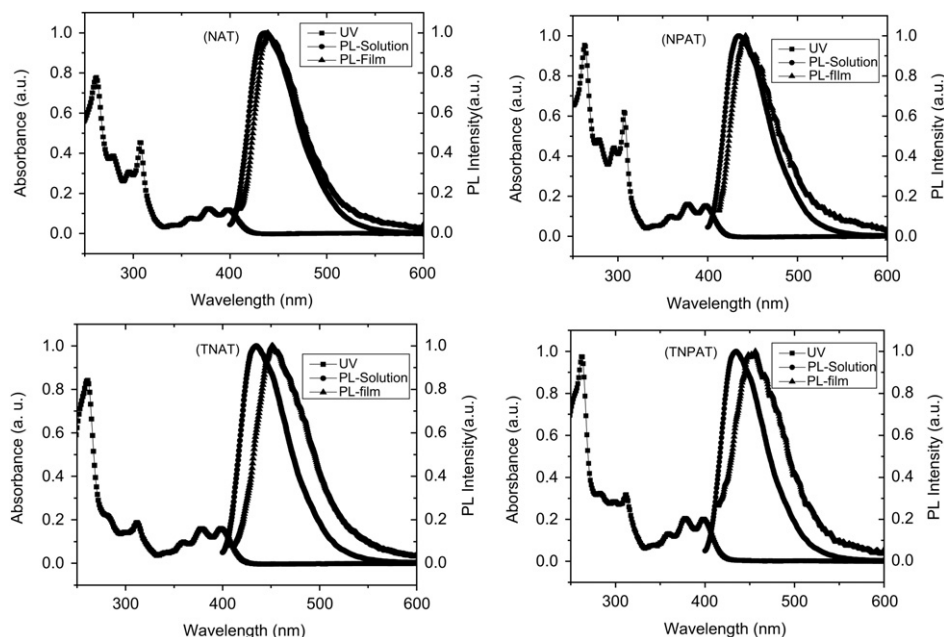


Figure 1. The absorbance spectra of anthracene derivatives in CH_2Cl_2 and PL spectra (excited at 380 nm) in CH_2Cl_2 and solid state.

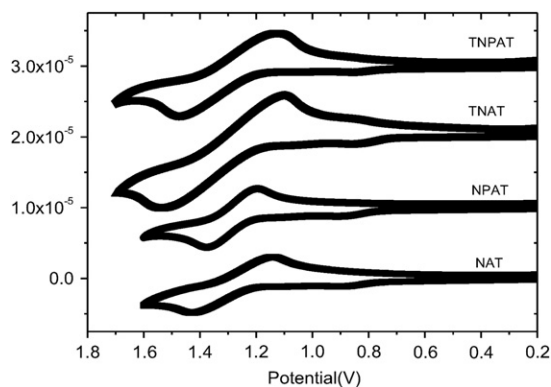


Figure 2. Cyclic voltammograms of NAT, NPAT, TNAT, and TNPAT in CH_2Cl_2 with 0.1 M Bu_4NPF_6 .

(1 nm)/Al (100 nm); **3** ITO/NPB (50 nm)/NPAT (40 nm)/TPBI (30 nm)/LiF (1 nm)/Al (100 nm); **4** ITO/NPB (50 nm)/NPAT (40 nm)/TPBI (15 nm)/LiF (1 nm)/Al (100 nm). CF_x was the hole-injection layer, 4,4'-bis[*N*-(1-naphthyl)-*N*-phenyl-*L*-amino]biphenyl (NPB) was used as the hole transporting layer, Alq_3 or TPBI was used as the electron transporting layer, and LiF was used as the electron injecting layer. The electroluminescent performance of the four devices was depicted in Table 2.

Table 2
Electroluminescent performance

Device	V_{on}^a	L_{max}^b (cd m^{-2})	λ_{em} (nm)	fwhm ^c (nm)	$\eta_{\text{c,max}}^d$ (cd A^{-1})	$\eta_{\text{p,max}}^e$ (lm/W)	CIE (x,y)
1	6.9	713	468	92	1.04	0.50	(0.18, 0.23)
2	6.5	508	456	72	1.3	0.93	(0.16, 0.15)
3	5.9	1318	460	72	2.98	1.52	(0.15, 0.14)
4	6.0	1288	448	68	2.1	1.02	(0.15, 0.10)

^a V_{on} , turn-on voltage.

^b L_{max} , maximum luminescence.

^c fwhm, full width at half maximum.

^d $\eta_{\text{c,max}}$, maximum current efficiency.

^e $\eta_{\text{p,max}}$, maximum power efficiency.

The I–V–L characteristics were also displayed in Figure 3. The devices exhibit better performance with TPBI as the electron transporting material than those with Alq_3 . The Alq_3 -based device with thin electron transporting material reveals the better performance than the thick device **1**, while the contrary case in the TPBI-based device. Thus, device **3** exhibited a maximum current efficiency of 2.98 cd A^{-1} (at 6.2 V) with a blue $\text{CIE}_{(x,y)}$ of (0.148, 0.138) and a maximum luminance of 1318 cd m^{-2} . At the same time, the $\text{CIE}_{(x,y)}$ of Alq_3 -based devices are more red-shifted as compared with the TPBI-based devices. This suggests that there is a contribution from the Alq_3 emission in the device **1** and **2**. The different emission zone found in the device **1–4** can be found due to the different HOMO and LUMO levels between the NPAT and Alq_3 or TPBI. Figure 4 revealed the identical electroluminescent spectra with a blue emission wavelength at 460 nm of device **3** at various applied current density from 1 mA/cm^2 to 100 mA/cm^2 . The result also implied the NPAT should be a potential candidate for stable blue host materials.

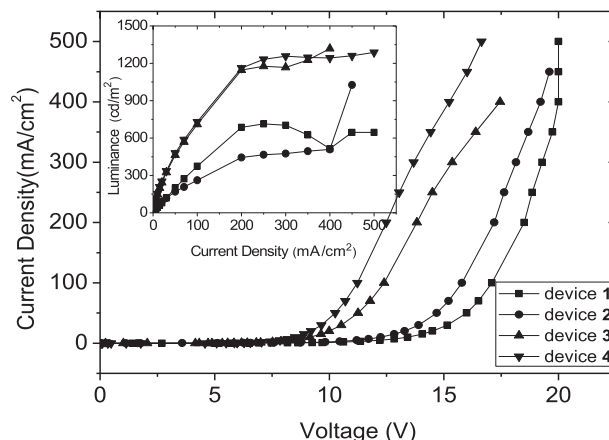


Figure 3. Current density–voltage–luminance of devices.

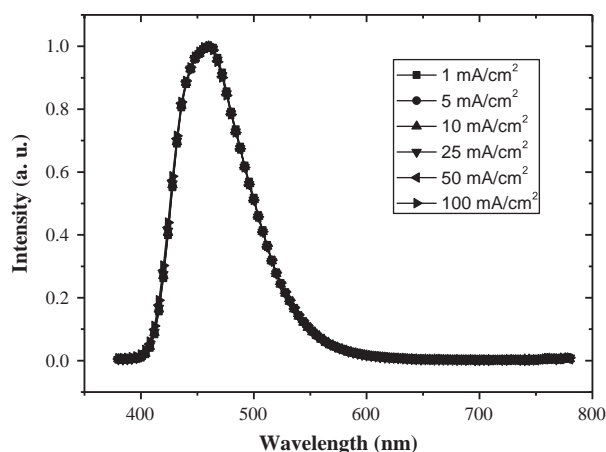


Figure 4. Electroluminescent spectra of device 3 at various applied current density.

3. Conclusions

In summary, we have synthesized four stable blue emission materials based on anthracene containing a truxene moiety as core. The measurements show these materials have good blue lighting performance with a good quantum yield. The PL spectra of three arms substituted truxene revealed more red-shift in the film than the single arm. The NPAT-based no-doped devices emit blue light. Moreover, the devices with TPBI as electron transporting material exhibit better performance than with Alq₃. A maximum current efficiency of 2.98 cd A⁻¹ and a maximum power efficiency of 1.52 lm/W at 6.2 V with a standard blue CIE_(x,y) of (0.148, 0.138) was achieved in the device structure of ITO/NPB (50 nm)/NPAT (40 nm)/TPBI (30 nm)/LiF (1 nm)/Al (100 nm).

4. Experimental

4.1. General information

Unless otherwise specified, all reactions and manipulations were performed under nitrogen atmosphere using standard Schlenk techniques. All chemical reagents were used as received from commercial sources without further purification. And the solvents were dried using standard procedures. ¹H and ¹³C NMR spectra were recorded on Brüker AV-400, spectrometer tetramethylsilane (TMS) as the internal standard. Mass spectrometric measurements were recorded by a LCT Premier XE mass spectrometry. High resolution mass spectrometric measurements were carried out using a Brüker autoflex MALDI-TOF mass spectrometer. UV–vis spectra were obtained on a Varian Cary 200 spectrophotometer. Fluorescence spectra were obtained on a Perkin–Elmer LS55 luminescence spectrometer. The differential scanning calorimetry (DSC) analysis was performed under a nitrogen atmosphere on a TA Instruments DSC 2920. The excitation was performed at 380 nm, and 9,10-diphenylanthracene (DPA) in the solution of cyclohexane, which has Φ_F=0.9, was used as a standard. Cyclic voltammetric (CV) measurements were carried out in a conventional three electrode cell using a Pt button working electrode of 2 mm in diameter, a platinum wire counter electrode, and a SCE reference electrode on a computer-controlled EG&G Potentiostat/Galvanostat model 283 at room temperature. Reduction CV of all compounds was performed in dichloromethane containing Bu₄NPF₆ (0.1 M) as the supporting electrolyte.

4.2. Device fabrication

Prior to the deposition of organic materials, indium–tin oxide (ITO)/glass was cleaned with a routine cleaning procedure and

pretreated with oxygen plasma. Devices were fabricated under about 10⁻⁶ Torr base vacuum in a thin-film evaporation coater. The current–voltage–luminance characteristics were measured with a diode array rapid scan system using a Photo Research PR650 spectrophotometer and a computer-controlled, programmable, direct-current (DC) source.

4.3. Synthesis

10-(2-Naphthyl)-9-bromoanthracene (**4a**)¹⁶ and 2,7,12-tri-bromo-5,5',10,10',15,15'-hexaethyltruxene (**7**)¹³ were synthesized in good yield according to the literatures.

4.3.1. Synthesis of 9-(4-(1-naphthyl)phenyl)anthracene (2b). A solution prepared by dissolving 4-(1-naphthyl)-phenyl boric acid (4.82 g, 19.53 mmol), 9-bromoanthracene (5 g, 19.43 mmol), tetrakis (triphenylphosphine) palladium(0) (0.5 g, 0.43 mmol), 40 ml THF, and potassium carbonate (2 M, 40 ml) were placed into 250 ml flask, and the residual mixture was heated to reflux for 24 h under N₂. After the reaction was completed, the reaction mixture was cooled to the room temperature, and formed crystals were separated by filtration. The obtained crystals were recrystallized from toluene, and 6.6 g of white crystals were obtained. Yield: 89.3%. ¹H NMR (400 Hz, CDCl₃, ppm): δ=8.48 (s, 1H), 8.11–8.14 (m, 1H), 8.02–8.04 (d, J=8.4 Hz, 2H), 7.87–7.93 (m, 2H), 7.79–7.81 (d, J=8.4 Hz, 2H), 7.66–7.68 (d, J=8.0 Hz, 2H), 7.36–7.59 (m, 10H). LCMS *m/z* [M+H]⁺: 381.1.

4.3.2. Synthesis of 10-(4-(1-naphthyl)phenyl)-9-bromoanthracene (3b). 9-(4-(1-Naphthyl)phenyl) anthracene (6.6 g, 17.37 mmol) and 120 ml of dehydrated dimethylformamide (DMF) were placed into a 250 ml flask, and the residual mixture was heated at 80 °C. After the material was dissolved, *N*-bromosuccinimide (NBS) (3.1 g, 17.37 mmol) was added at 50 °C, and the reaction mixture was stirred for 10 h. After the reaction was completed, the reaction solution was poured into 300 ml of purified water, and formed crystals were separated by filtration. The separated crystals were recrystallized from toluene, and 6.3 g of yellow crystals were obtained. Yield: 79.2%. ¹H NMR (400 Hz, CDCl₃, ppm): δ=8.57–8.59 (d, J=8.4 Hz, 1H), 8.07–8.10 (m, 1H), 7.85–7.91 (m, 2H), 7.75–7.77 (d, J=8.8 Hz, 2H), 7.65–7.69 (d, J=8.4 Hz, 2H), 7.54–7.58 (m, 4H), 7.45–7.450 (m, 4H), 7.37–7.41 (m, 2H). ¹³C NMR (CDCl₃, 400 MHz, ppm): δ 140.00, 139.65, 137.35, 137.10, 133.74, 131.42, 130.93, 130.88, 130.10, 129.92, 129.85, 128.24, 127.73, 127.25, 126.98, 126.81, 126.01, 125.79, 125.71, 125.46, 125.28, 122.67. LCMS *m/z* [M+H]⁺: 459.0.

4.3.3. Synthesis of 10-(4-(1-naphthyl)phenyl)-anthracene-9-boric acid (4b). 10-(4-(1-Naphthyl)phenyl)-9-bromoanthracene (3 g, 6.55 mmol) was added to 80 ml of dry THF solution and stirred for 30 min at -78 °C, then *n*-BuLi (4.0 ml, 9.83 mmol, 2.5 M solution in hexane) was added. The mixture was stirred at room temperature for 2 h. After the reaction was cooled to -78 °C, trimethylborate (1.51 ml, 12.87 mmol) was added to the reaction mixture. After the addition was completed, the solution was warmed slowly to room temperature and then stirred for 12 h. The reaction mixture was added to an aqueous solution of HCl (2 N) and extracted with diethyl ether. The organic extracts were washed with brine and water, and dried with anhydrous MgSO₄, and filtered. After the solvent was evaporated, the crude product was purified by column chromatography with petroleum ether/ethyl acetate=3:1 eluent to afford a 1.65 g of yellow powder. Yield: 59.4%. ¹H NMR (400 MHz, CDCl₃, ppm): δ=8.18–8.23 (m, 3H), 7.95–8.01 (m, 2H), 7.87–7.90 (d, J=8.8 Hz, 2H), 7.75–7.77 (d, J=8.8 Hz, 2H), 7.64–7.66 (m, 2H), 7.55–7.60 (m, 6H), 7.45–7.55 (m, 2H), 5.25 (s, 2H). ¹³C NMR (DMSO, 400 MHz, ppm): δ 139.25, 137.53, 135.68, 133.57, 132.38, 131.01,

130.93, 130.00, 129.49, 129.15, 128.46, 127.84, 127.14, 126.55, 126.47, 126.05, 125.68, 125.55, 125.39, 124.82.

4.3.4. Synthesis of 2-iodo-5,5',10,10',15,15'-hexaethyltruxene (5). A mixture of truxene (3.5 g, 6.86 mmol) and 15 ml solvent ($\text{CH}_3\text{COOH}:\text{H}_2\text{SO}_4:\text{H}_2\text{O}:\text{CCl}_4=100:5:20:8$) was heated to 40 °C. After adding HIO_3 (0.40 g, 2.29 mmol) and I_2 (0.58 g, 2.29 mmol) to the mixture, the mixture was heated to 80 °C and stirred for 4 h at this temperature. After the reaction was completed, the mixture was cooled to room temperature and filtered off under suction, washed with water. Then the residue refluxed in methanol for 2 h and followed by cooling to room temperature, filtered off under suction, and 3.0 g of white powder was afforded. Yield: 68.8%. ^1H NMR (CDCl_3 , 400 MHz, ppm) $\delta=8.25\text{--}8.31$ (m, 2H), 8.03–8.05 (d, $J=8.4$ Hz, 1H), 7.65–7.72 (m, 2H), 2.83–3.10 (m, 6H), 2.02–2.12 (m, 6H), 0.13–0.17 (m, 18H). ^{13}C NMR (CDCl_3 , 400 MHz, ppm): δ 155.61, 152.97, 152.81, 144.76, 144.20, 143.37, 140.60, 140.52, 140.49, 139.29, 139.02, 138.03, 135.37, 131.69, 126.38, 124.81, 124.74, 124.66, 122.51, 122.45, 92.42, 57.18, 56.99, 56.87, 29.60, 29.54, 29.48, 8.72, 8.68. LCMS m/z [$\text{M}+\text{H}$] $^+$: 637.1.

4.3.5. Synthesis of NTA. A solution prepared by dissolving 10-(2-naphthyl) anthracene-9-boric acid (0.348 g, 1.0 mmol), 2-iodo-5,5',10,10',15,15'-hexaethyltruxene (0.636 g, 1.0 mmol), tetrakis(triphenylphosphine) palladium (0) (100 mg, 0.09 mmol), 20 ml of THF, and potassium carbonate (2 M, 20 ml) were placed into 100 ml flask, and residual mixture was stirred for 24 h while being heated under the refluxing condition. After the reaction was completed, the reaction mixture was cooled to the room temperature, and the mixture was extracted with 20 ml CH_2Cl_2 solution three times. The organic portion was combined and removed by rotary evaporation. The residue was purified by column chromatography with silica gel using hexane and CH_2Cl_2 (4:1) as eluent to afford 0.5 g of yellow solid. Yield: 61.6%. ^1H NMR (400 Hz, CDCl_3): $\delta=8.58\text{--}8.56$ (d, $J=8.0$ Hz, 1H), 8.36–8.42 (m, 2H), 8.09–8.11 (d, $J=8.0$ Hz, 2H), 7.00–8.05 (m, 3H), 7.90–7.95 (m, 3H), 7.75–7.77 (d, $J=8.0$ Hz, 2H), 7.32–7.68 (m, 15H), 3.05–3.20 (m, 6H), 2.13–2.26 (m, 6H), 0.25–0.42 (m, 18H). ^{13}C NMR (CDCl_3 , 400 MHz, ppm): δ 152.97, 152.88, 152.82, 144.19, 144.10, 144.07, 140.71, 140.59, 140.05, 139.01, 138.90, 138.70, 137.71, 137.07, 136.85, 136.63, 133.41, 132.75, 130.26, 130.11, 130.06, 129.59, 129.22, 128.11, 128.00, 127.92, 127.13, 127.08, 126.53, 126.44, 126.23, 126.13, 125.45, 125.13, 124.75, 124.766, 124.60, 122.3, 56.89, 56.84, 56.79, 29.549, 29.44, 29.38, 8.73, 8.62. MALDI-TOF-MS m/z calculated for $\text{C}_{63}\text{H}_{56}$: 812.4382, found [M^+]: 812.4408, [$\text{M}-\text{CH}_3\text{CH}_2$] $^+$: 783.4131.

4.3.6. Synthesis of NPAT. A solution prepared by dissolving 10-(4-(1-naphthyl)phenyl)-anthracene-9-boric acid (0.424 g, 1.0 mmol), 2-iodo-5,5',10,10',15,15'-hexaethyltruxene (0.636 g, 1.0 mmol), tetrakis(triphenylphosphine)palladium(0) (100 mg, 0.09 mmol), 20 ml THF, and potassium carbonate (2 M, 20 ml) were placed into 100 ml flask, and residual mixture was stirred for 24 h while being heated under the refluxing condition. After the reaction was completed, the reaction mixture was cooled to the room temperature, and the mixture was extracted with 20 ml CH_2Cl_2 solution three times. The organic portion was combined and removed by rotary evaporation. The residue was purified by column chromatography with silica gel using hexane and methylene chloride (4:1) as eluent to afford 0.44 g of yellow solid. Yield: 50%. ^1H NMR (400 Hz, CDCl_3 , ppm): $\delta=8.56\text{--}8.58$ (d, $J=8.4$ Hz, 1H), 8.37–8.42 (m, 2H), 8.20–8.22 (m, 1H), 7.91–8.00 (m, 6H), 7.77–7.79 (d, $J=8.0$ Hz, 2H), 7.38–7.68 (m, 18H), 3.05–3.20 (m, 6H), 2.14–2.27 (m, 6H), 0.25–0.42 (m, 18H). ^{13}C NMR (CDCl_3 , 400 MHz, ppm): δ 153.01, 152.91, 152.86, 144.23, 144.15, 144.12, 140.74, 140.62, 140.08, 139.93, 139.06, 138.95, 138.74, 138.08, 137.70, 137.13, 136.84, 133.97, 131.71, 131.31, 130.14, 130.10, 129.25, 128.43, 127.83, 127.21, 127.17, 127.11, 126.58, 126.20, 126.14, 125.91, 125.52,

125.19, 124.76, 124.69, 124.61, 122.36, 56.93, 56.88, 56.82, 29.54, 29.47, 29.42, 8.73, 8.61. MALDI-TOF-MS m/z calculated for $\text{C}_{69}\text{H}_{60}$: 888.4695, found [M^+]: 888.4711, [$\text{M}-\text{CH}_3\text{CH}_2$] $^+$: 859.4452.

4.3.7. Synthesis of TNAT. A solution prepared by dissolving 10-(2-naphthyl) anthracene-9-boric acid (0.63 g, 1.8 mmol), 2,7,12-tribromo-5,5',10,10',15,15'-hexaethyltruxene (0.374 g, 0.5 mmol), tetrakis(triphenylphosphine) palladium (0) (100 mg, 0.09 mmol), 20 ml THF, and potassium carbonate (2 M, 20 ml) were placed into 100 ml flask, and residual mixture was stirred and heated to refluxed for 24 h. After the reaction was completed, the reaction mixture was cooled to the room temperature, and the mixture was extracted with 20 ml CH_2Cl_2 solution three times. The organic portion was combined and removed by rotary evaporation. The residue was purified by column chromatography with silica gel using hexane and CH_2Cl_2 (4:1) as eluent to afford 0.51 g of yellow solid. Yield: 72%. ^1H NMR (400 Hz, CDCl_3 , ppm): $\delta=8.64\text{--}8.66$ (d, $J=8.4$ Hz, 3H), 8.11–8.13 (d, $J=8.4$ Hz, 3H), 8.02–8.07 (m, 6H), 7.95–7.97 (m, $J=8.4$ Hz, 9H), 7.77–7.79 (d, $J=8.8$ Hz, 6H), 7.56–7.69 (m, 15H), 7.42–7.46 (m, 6H), 7.35–7.37 (m, 6H), 3.28–3.33 (m, 6H), 2.27–2.32 (m, 6H), 0.57–0.60 (m, 18H). ^{13}C NMR (CDCl_3 , 400 MHz, ppm): δ 153.02, 144.63, 140.04, 138.94, 137.69, 137.25, 136.90, 136.62, 133.41, 132.75, 130.26, 130.12, 130.08, 129.59, 129.32, 128.11, 128.01, 127.92, 127.14, 127.11, 126.45, 126.24, 125.55, 125.17, 124.86, 57.07, 29.53, 8.99. MALDI-TOF-MS m/z calculated for $\text{C}_{111}\text{H}_{84}$: 1417.6607, found [M^+]: 1417.6582, [$\text{M}-\text{CH}_3\text{CH}_2$] $^+$: 1388.6068.

4.3.8. Synthesis of TNPAT. A solution prepared by dissolving 10-(4-(1-naphthyl) phenyl)-anthracene-9-boric acid (0.9 g, 2.12 mmol), 2,7,12-tribromo-5,5',10,10',15,15'-hexaethyltruxene (0.44 g, 0.59 mmol), tetrakis(triphenylphosphine) palladium(0) (100 mg, 0.09 mmol), 20 ml THF, and potassium carbonate (2 M, 20 ml) were placed into 100 ml flask, and residual mixture was stirred for 24 h while being heated under the refluxing condition. After the reaction was completed, the reaction mixture was cooled to the room temperature, and the mixture was extracted with 20 ml CH_2Cl_2 solution three times. The organic portion was combined and removed by rotary evaporation. The residue was purified by column chromatography with silica gel using hexane and CH_2Cl_2 (4:1) as eluent to afford 0.47 g of yellow solid. Yield: 48.5%. ^1H NMR (400 Hz, CDCl_3 , ppm): $\delta=8.64\text{--}8.66$ (d, $J=8.0$ Hz, 3H), 8.22–8.23 (m, 3H), 7.92–8.00 (m, 18H), 7.77–7.79 (d, $J=8.0$ Hz, 6H), 7.56–7.69 (m, 24H), 7.46–7.48 (m, 12H), 3.29–7.34 (m, 6H), 2.28–2.33 (m, 6H), 0.58–0.62 (m, 18H). ^{13}C NMR (CDCl_3 , 400 MHz, ppm): δ 153.17, 144.80, 140.19, 140.06, 139.10, 138.18, 137.79, 137.44, 137.00, 134.07, 131.82, 131.43, 130.28, 130.23, 129.47, 128.54, 127.94, 127.31, 127.24, 126.31, 126.24, 126.01, 125.74, 125.62, 125.32, 124.98, 57.23, 29.68, 9.10. MALDI-TOF-MS m/z calculated for $\text{C}_{129}\text{H}_{96}$: 1645.7546, found [M^+]: 1645.7548, [$\text{M}-\text{CH}_3\text{CH}_2$] $^+$: 1616.7027.

Acknowledgements

This work was financially supported by NSFC/China, National Basic Research 973 Program.

Supplementary data

This section contains the TGA analysis and ^1H NMR and ^{13}C NMR spectra of the synthesized compounds. Supplementary data associated with this article can be found in online version at doi:10.1016/j.tet.2010.07.039.

References and notes

- (a) Tang, C. W.; Van Slyke, S. A. *Appl. Phys. Lett.* **1987**, *51*, 913–915; (b) Burroughes, J. H.; Bradley, D. D. C.; Brown, A. R.; Marks, R. N.; Mackay, K.; Friend, R. H.; Burns,

- P. L.; Holmes, A. B. *Nature* **1990**, *347*, 539–541; (c) Kido, J.; Kimura, M.; Nagai, K. *Science* **1995**, *267*, 1332–1334; (d) Tasch, S.; List, E. J. W.; Wkström, O.; Graupner, W.; Leisting, G.; Schlichting, P.; Rohr, U.; Greerts, Y.; Scherf, U.; Müllen, K. *Appl. Phys. Lett.* **1997**, *71*, 2883–2885; (e) Kraft, A.; Grimsdale, A. C.; Holmes, A. B. *Angew. Chem., Int. Ed.* **1998**, *37*, 402–428; (f) Huang, L. S.; Chen, C. H. *Mater. Sci. Eng. R* **2002**, *39*, 143–222; (g) Wu, H. B.; Zhou, G. J.; Zou, J. H.; Ho, C.-L.; Wong, W.-Y.; Yang, W.; Peng, J. B.; Cao, Y. *Adv. Mater.* **2009**, *21*, 4181–4184.
2. Tang, C. W.; Van Slyke, S. A.; Chen, C. H. *J. Appl. Phys.* **1989**, *65*, 3610–3616.
 3. (a) Gao, Z. Q.; Mi, B. X.; Chen, C. H.; Cheah, K. W.; Cheng, Y. K.; Wen, W. S. *Appl. Phys. Lett.* **2007**, *90*, 123506-1–123506-3; (b) Kim, Y.-H.; Jeong, H.-C.; Kim, S.-H.; Yang, K. Y.; Kwon, S.-K. *Adv. Funct. Mater.* **2005**, *15*, 1799–1805; (c) Lyu, Y.-Y.; Kwak, J. H.; Kwon, O. Y.; Lee, S.-H.; Kim, D. Y.; Lee, C. H.; Char, K. *Adv. Mater.* **2008**, *20*, 2720–2729; (d) Culligan, S. W.; Chen, A. C.-A.; Wallace, J. U.; Klubek, K. P.; Tang, C. W.; Chen, S. H. *Adv. Funct. Mater.* **2006**, *16*, 1481–1487; (e) Kim, S.-K.; Yang, B.; Ma, Y. G.; Lee, J.-H.; Park, J. W. *J. Mater. Chem.* **2008**, *18*, 3376–3384; (f) Danel, K.; Huang, T.-H.; Lin, J. T.; Tao, Y.-T.; Chuen, C.-H. *Chem. Mater.* **2002**, *14*, 3860–3865; (g) Sun, J.; Zhong, H. L.; Xu, E. J.; Zeng, D. L.; Zhang, J. H.; Xu, H. G.; Zhu, W. Q.; Fang, Q. *Org. Electron.* **2010**, *11*, 74–80.
 4. Wu, C.-H.; Chien, C.-H.; Hsu, F.-M.; Shih, P.-I.; Shu, C.-F. *J. Mater. Chem.* **2009**, *19*, 1464–1470.
 5. Xia, Z.-Y.; Zhang, Z.-Y.; Su, J.-H.; Zhang, Q.; Fuang, K.-M.; Lam, M.-K.; Li, K.-F.; Wong, W.-Y.; Cheah, K. W.; Tian, H.; Chen, C. H. *J. Mater. Chem.* **2010**, *20*, 3768–3774.
 6. Gomez-Lor, B.; Defrutos, O.; Ceballos, P. A.; Granier, T.; Echavarren, A. M. *Eur. J. Org. Chem.* **2001**, 2107–2114.
 7. (a) Cao, X.-Y.; Liu, X.-H.; Zhang, Y.; Jiang, Y.; Cao, Y.; Cui, Y.-X.; Pei, J. *J. Org. Chem.* **2004**, *69*, 6050–6058; (b) Luo, J.; Zhou, Y.; Niu, Z.-Q.; Zhou, Q.-F.; Ma, Y. G.; Pei, J. *J. Am. Chem. Soc.* **2007**, *129*, 11314–11315; (c) Lai, W.-Y.; Xia, R.; He, Q.-Y.; Levermore, P. A.; Huang, W.; Bradley, D. D. C. *Adv. Mater.* **2008**, *20*, 1–6; (d) Yuan, S.-C.; Sun, Q. J.; Lei, T.; Du, B.; Li, Y.-F.; Pei, J. *Tetrahedron* **2009**, *65*, 4165–4172; (e) Yang, Z. F.; Xu, B.; He, J. T.; Xue, L. L.; Guo, Q.; Xia, H. J.; Tian, W. J. *Org. Electron.* **2009**, *10*, 954–959; (f) Lei, T.; Luo, J.; Wang, L.; Ma, Y. G.; Wang, J.; Cao, Y.; Pei, J. *New J. Chem.* **2010**, *34*, 699–707; (g) Jiang, Y.; Wang, L.; Zhou, Y.; Cui, Y.-X.; Wang, J.; Cao, Y.; Pei, J. *Chem.—Asian J.* **2009**, *4*, 548–553.
 8. (a) Perova, T. S.; Vij, J. K. *Adv. Mater.* **1995**, *7*, 919–922; (b) Sandstroem, D.; Nygren, M.; Zimmermann, H.; Maliniak, A. *J. Phys. Chem.* **1995**, *99*, 6661–6669; (c) Fontes, E.; Herney, P. A.; Ohba, M.; Haseltine, J. N.; Smith, A. B. *Phys. Rev. A* **1988**, *37*, 1329–1334.
 9. (a) Lai, W. Y.; Xia, R.; He, Q.; Levermore, P. A.; Huang, W.; Bradley, D. D. C. *Adv. Mater.* **2009**, *21*, 355–360; (b) Zhou, X.; Feng, J.-K.; Ren, A.-M. *Synth. Met.* **2005**, *155*, 615–617.
 10. Yuan, M.-S.; Liu, Z.-Q.; Fang, Q. *J. Org. Chem.* **2007**, *72*, 7915–7922.
 11. Ning, Z. J.; Zhang, Q.; Pei, H. C.; Luan, J. F.; Lu, C. G.; Cui, Y. P.; Tian, H. J. *Phys. Chem. C* **2009**, *113*, 10307–10313.
 12. (a) Xia, H. J.; He, J. T.; Xu, B.; Wen, S. P.; Li, Y. W.; Tian, W. J. *Tetrahedron* **2008**, *64*, 5736–5742; (b) Kanibolotsky, A. L.; Berridge, R.; Skabara, P. J.; Perepichka, I. F.; Bradley, D. D. C.; Koeberg, M. *J. Am. Chem. Soc.* **2004**, *126*, 13695–13702; (c) Wang, J.-L.; Yan, J.; Tang, Z. M.; Xiao, Q.; Ma, Y. G.; Pei, J. *J. Am. Chem. Soc.* **2008**, *130*, 9952–9962.
 13. Yuan, M.-S.; Fang, Q.; Liu, Z.-Q.; Guo, J.-P.; Chen, H.-Y.; Yu, W.-T.; Xue, G.; Liu, D.-S. *J. Org. Chem.* **2006**, *71*, 7858–7861.
 14. Salbeck, J.; Weissörtel, F.; Yu, N.; Baner, J.; Bestgen, H. *Synth. Met.* **1997**, *91*, 209–215.
 15. Kim, S.-K.; Park, Y.; Kang, I.-N.; Park, J.-W. *J. Mater. Chem.* **2007**, *17*, 4670–4678.
 16. Wang, L.; Wong, W.-Y.; Lin, M.-F.; Wong, W.-K.; Cheah, K.-W.; Tam, H.-L.; Chen, C. H. *J. Mater. Chem.* **2008**, *18*, 4529–4536.